JOURNAL OF GEOPHYSICAL RESEARCH, VOL. 92, NO. C13, PAGES 14,189–14,196, DECEMBER 15, 1987

El Niño Events and Their Relation to the Southern Oscillation: 1925–1986

CLARA DESER AND JOHN M. WALLACE

Department of Atmospheric Sciences, University of Washington, Seattle

Relationships among sea surface temperatures (SSTs) at the coast of Peru and offshore, river discharge in northern Peru, and sea level pressure at Darwin, Australia, during the period 1925–1986 are investigated using time series plots, frequency distributions, and a simple statistical analysis. It is shown that SSTs undergo a larger seasonal cycle offshore than at the coast, exhibit more interannual variability during the warm than the cool season, are positively skewed during much of the year, and exhibit greatest month-to-month persistence during the cool season. Many, but not all, episodes of above normal coastal SSTs are accompanied by enhanced river discharge in northern Peru. Comparison of the Darwin pressure and coastal SST records during the past 60 years shows that El Niño events (episodes of above normal SSTs along the coast of Peru) have occurred both in advance of and subsequent to major negative swings of the Southern Oscillation (and associated climatic changes in the central equatorial Pacific). In addition, El Niño events and negative swings of the Southern Oscillation have occurred separately. Hence El Niño and the Southern Oscillation are more loosely coupled than other studies would imply.

1. INTRODUCTION

The El Niño phenomenon along the coast of northern Peru and southern Ecuador and the Pacific-wide Southern Oscillation phenomenon were discovered independently, and until the 1960s, they were considered unrelated. *Carillo* [1892] ascribed the term El Niño to Peruvian mariners who used the title to refer to a warm narrow countercurrent flowing southward along the northern coast of Peru shortly after Christmastime. As such, El Niño was originally viewed as an annual event, although the strength and southernmost extent of this countercurrent were observed to vary from year to year [*Eguiguren*, 1894]. In his investigation of the interannual variability of the rains at Piura in northern coastal Peru, Eguiguren hypothesized that the enhanced precipitation observed during some rainy seasons is due to an unusually well developed countercurrent. He noted that weakened coastal southerly surface winds would aid the development of the El Niño current. *Murphy* [1926] documented the torrential rains and unusually strong countercurrent along coastal Peru and southwestern Ecuador during the first few months of 1925. *Lobell* [1942] found anomalously warm surface temperatures in the Peruvian coastal waters during early 1941 but no evidence of a southward flowing countercurrent. He concluded that warm water was advected onshore, a condition brought about by a shift in the prevailing winds. *Schweigger* [1945] proposed that large-scale southeastward advection of warm water from around the Galapagos Islands is responsible for the major climatic changes previously attributed to the El Niño current. However, the use of the term El Niño to describe the occasional appearance of excessively warm water along the coast of northern Peru and southern Ecuador extending westward to the Galapagos Islands was already widespread [see *Schott*, 1931; *Gunther*, 1936; *Mears* 1943]. *Wooster* [1960] and *Bjerknes* [1961] hypothesized that warming of the coastal waters is due to a weakening of the northward component of the wind stress along the coast, reducing upwelling, allowing warmer waters offshore to approach the coast, and allowing the coastal countercurrent to penetrate further south. According to this hypothesis, "a strong El Niño would represent nothing but an amplification of the [normal] summer warming" [*Wyrtki*, 1975]. Wyrtki subsequently disproved this hypothesis by showing that the coastal southerlies actually tend to be slightly stronger than normal during El Niño events. *Quinn et al.* [1978] provided the first comprehensive documentation on past El Niño events, including statistics on intensity, duration, and frequency of occurrence; this work has recently been revised and updated [see *Quinn*, this issue].

The Southern Oscillation refers to the seesaw in surface pressure anomalies between the Indian Ocean–Australian region and the southeastern tropical Pacific on seasonal time scales. The Southern Oscillation was first documented in the works of *Hildebrandsson* [1897] and *Lockyer and Lockyer* [1904] and was clearly identified in the landmark paper of *Walker and Bliss* [1932], who recognized its relation to a complex pattern of pressure, temperature, and rainfall anomalies encompassing much of the globe. Subsequent studies by *Troup* [1965], *Berlage* [1966], *Kidson* [1975], *Trenberth* [1976], *Barnett* [1985], and many others have confirmed the relationships identified by Walker and Bliss and have added many important details. The idea of alternating strengthening and weakening of the southeast trades and the equatorial easterlies in the Pacific, first noted by *Brooks and Braby* [1921], has come to be regarded as central to the concept of the Southern Oscillation.

Bjerknes [1966] postulated that weakening of the equatorial easterlies across the eastern half of the Pacific that occurs in association with negative swings of the Southern Oscillation (i.e., pressure rises over Australia and Indonesia and falls over the subtropical southeast Pacific) reduces equatorial upwelling in the eastern Pacific and thereby leads to an increase of SST. Bjerknes used the term El Niño, which had previously been used exclusively in association with the SST increases along the Peru and Ecuador coast, as a label for this much broader-scale phenomenon, and this usage has been subsequently adopted by *Wyrtki* [1975] and many other authors. In the present study, we adhere to the classical definition of El Niño as a warming of the coastal waters off Peru and Ecuador.

Wyrtki [1975] postulated that the initial increase of SST

Paper number 7C0605.
0148-0227/87/007C-0605$05.00

along the coast of northern Peru is a remote response to a sudden relaxation of the equatorial winds in the central and western Pacific. The increase in SST in the eastern equatorial Pacific leads to a reduction of the atmospheric surface pressure gradient across the Pacific which further weakens the equatorial zonal winds. The dynamic coupling of El Niño and the Southern Oscillation has been confirmed by the results of equatorial ocean models (for example, see the review by *Cane* [1983]), which have proved to be capable of simulating many aspects of the observed changes in sea level, sea surface temperature (SST), equatorial currents, and thermocline depth that occur in association with El Niño events.

Rasmusson and Carpenter [1982] carried the synthesis of El Niño and the Southern Oscillation phenomenon a step further by presenting a Pacific-wide composite based on six El Niño events along the Peru coast during the period 1950–1975. Their study has provided what has come to be known as the canonical El Niño–Southern Oscillation event, characterized by (1) strong positive SST anomalies extending from the Galapagos Islands eastward to the south American coast during January–May and weaker but spatially coherent warming of SST extending across the entire equatorial Pacific east of 170°E peaking around October, (2) heavy rainfall along the Peru coast and over the central equatorial Pacific, and (3) a pronounced negative swing of the Southern Oscillation. The concept of El Niño and the Southern Oscillation as a coupled phenomenon has gained such wide acceptance that the acronym ENSO (El Niño–Southern Oscillation), used extensively in the Rasmusson and Carpenter paper, has been widely adopted as a label for large scale atmosphere-ocean interaction in the tropical Pacific, and it has even been used as a name for specific episodes of positive SST anomalies [*Fu et al.*, 1986].

In the present study we will take a more critical look at the relationships involved in the El Niño phenomenon along the coast of Peru. Specifically, we will consider the increase of SST and the enhancement of rainfall along the northern Peru coast. In contrast to the works of *Wyrtki* [1975] and *Rasmusson and Carpenter* [1982], which focussed on El Niño events during the 1950–1975 period, we examine 60 years of SST data from ship reports and a coastal station. We also make use of a newly available time series of river discharge in northern Peru. We will show that when the full 60-year record is taken into account, the relationships between El Niño and the Southern Oscillation are not as strong and as straightforward as might be inferred from previous studies encompassing the two phenomena.

2. Coastal Versus Offshore SST

Time series of monthly mean SST for Puerto Chicama (8°S, 80°W) and the shipping lane along the coast of northern Peru were provided by E. Rasmusson of the University of Maryland, College Park. The ship track data, hereafter referred to as "offshore", represent the average SST for latitudes 4°–12°S, between the coast and approximately 5° of longitude offshore. The offshore SST series for the periods of 1921–1938 and 1949–1976 were presented by Rasmusson and Carpenter [1982] (their SST1); the series we are using has been updated to July 1986. The SST record for Puerto Chicama covers the period January 1925 through June 1986. SST anomalies at Puerto Chicama are well correlated with those at other coastal sites between 4°S and 12°S; in particular, the correlation coefficients between monthly SST anomalies (smoothed with a three-point binomial filter) at Puerto Chicama and Talara (4.5°S) and at Puerto Chicama and Callao (12°S) are 0.84 and 0.90, respectively, for the period 1950–1979. Puerto Chicama is the only coastal site between 4°S and 12°S providing SST data since the 1920s; other coastal SST records begin in the late 1940s. In this section, we compare Puerto Chicama and offshore SSTs by examining their frequency distributions as a function of month (Figures 1 and 2). Table 1 provides more quantitative information on the frequency distributions, i.e., means, standard deviations, and skewness coefficients as a function of calendar month. Unless otherwise noted, the results for Puerto Chicama SSTs are corroborated by the shorter SST records at other coastal sites between 4°S and 12°S.

SST is generally lower at Puerto Chicama than offshore throughout the year, despite the fact that the mean latitude of the ship track coincides with the location of the coastal station (8°S). In fact, the annual mean SST is higher offshore than at any coastal station between 4°S and 12°S [*Lagos et al.*, this issue]. The average difference between SST at Puerto Chicama and offshore ranges from around 2.5°C during July–September to over 5.0°C during the warm season, January–April. The relative coolness of the nearshore surface water is

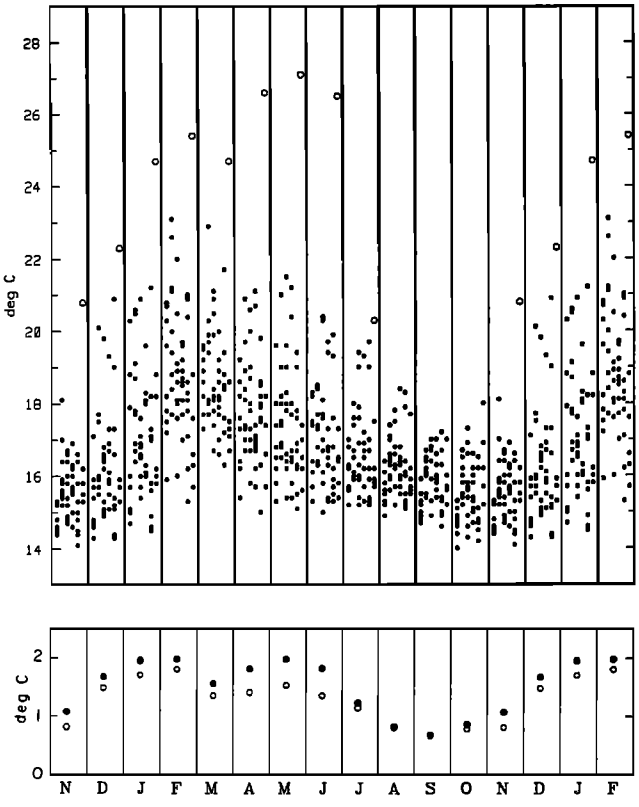

Fig. 1. (top) Distribution of SST (in degrees Celsius) at Puerto Chicama (8°S, 80°W) during 1931–1986, stratified by month. Each dot marks the mean SST for an individual year-month. Each column of dots within a given calendar month represents a particular decade; i.e., the first (last) column of dots contains data for the 1930s (1980s). November through February are repeated. Data for November 1982 through July 1983 are marked by open circles. (bottom) Standard deviation (in degrees Celsius) of SST anomalies at Puerto Chicama, stratified by month. Dots represent values based on the period 1931–1986; open circles denote values based on the periods 1931–1981 and 1984–1986.

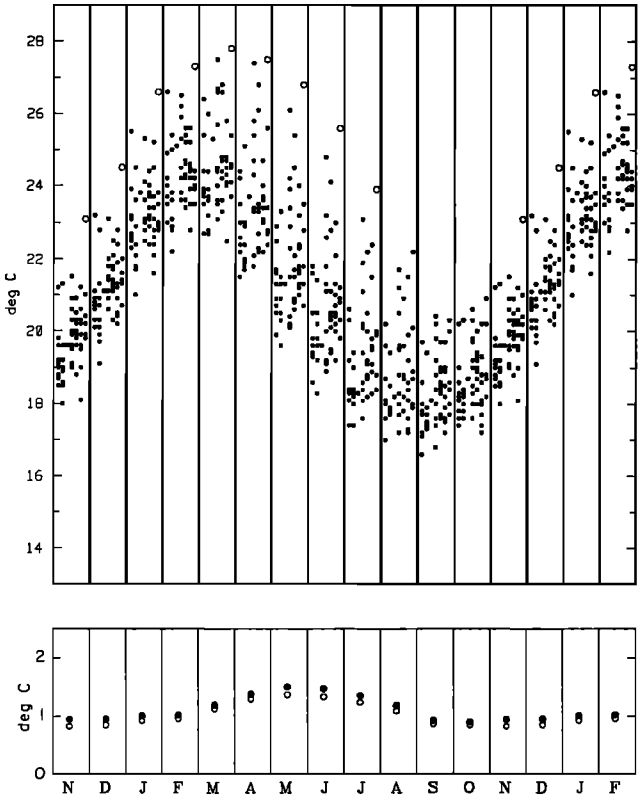

Fig. 2. As in Figure 1 but for offshore SST during 1921–1939 and 1948–1986. (Offshore SST is the average SST in the region 4°S to 12°S, within 5° of longitude of the coast.) Standard deviations are based on the periods 1921–1939 and 1948–1986 (dots) and 1921–1939, 1948–1981, and 1984–1986 (open circles).

primarily due to coastal upwelling, which along the coast of Peru between 4°S and 12°S is confined to within about 50 km of the shore [*Smith*, 1981; *Guillén and Calienes*, 1981].

The annual range of SST averages about 6°C offshore, nearly twice the amplitude at Puerto Chicama. In fact, offshore SSTs exhibit a substantially larger annual cycle than do SSTs from any coastal station between 2°S and 15°S [see *Lagos et al.*, this issue]. This difference in amplitude is particularly pronounced for the cold limit of the SST "envelope" which undergoes only a small (2°C) annual variation at Puerto Chicama versus a 5°C annual variation offshore. (In 1950 and 1981 the annual range of SST at Puerto Chicama was only 1.8°C.) The reduction of the mean annual range of SST at the coast of Peru relative to that several hundred kilometers offshore may be, in part, a direct consequence of the narrow horizontal scale of the coastal upwelling. The surface water within the narrow coastal upwelling zone originates from between 20-m and 40-m depth where the annual temperature variation is relatively weak.

It is apparent from Figures 1 and 2 that the shape of the mean annual SST curve is markedly different at Puerto Chicama than offshore. The mean seasonal cycle of offshore SST can be closely approximated by a single harmonic, with warming from September to March and cooling during the rest of the year. However, at Puerto Chicama the mean seasonal cycle is asymmetric, with rapid warming from November to February and more gradual cooling from February to October. SSTs at other coastal stations between 2°S and 15°S do not exhibit such pronounced asymmetry of the annual cycle [*Lagos et al.*, this issue].

As can be seen from Figures 1 and 2, SSTs tend to exhibit larger dispersion about the monthly means at Puerto Chicama than offshore. In particular, the 1982–1983 temperature anomalies, highlighted in the figures, were far more extreme at Puerto Chicama than offshore. The monthly standard deviations of the SST anomalies, which are a measure of interannual variability, are shown in the bottom panels of Figures 1 and 2. (The standard deviations of the SST anomalies computed without data for 1982–1983 are also shown in Figures 1 and 2.) Both time series exhibit pronounced seasonal variations in standard deviation, with a maximum in May and a minimum around October. In addition, Puerto Chicama SST exhibits a second maximum in standard deviation during January–February, when the standard deviation of offshore SST is near a minimum. This distinction between the two SST series is even apparent in the frequency distributions themselves. *Rasmusson and Carpenter* [1982] noted that the behavior of SST offshore and at Puerto Chicama was markedly different during the tail end (January–February) of major El Niño events: a second anomaly maximum during January–February was prominent at Puerto Chicama but was barely detectable in offshore SST.

We have computed the monthly standard deviations of SST for non–El Niño years separately (not shown) and found a similar, albeit less pronounced, pattern of seasonal variation. In particular, for Puerto Chicama SST, the maximum standard deviation is reduced from 1.8°C to 1.3°C while the minimum standard deviation falls from 0.6°C to 0.5°C when El Niño years are excluded from the calculation.

TABLE 1. Moment Statistics for SST Anomalies

	Jan.	Feb.	March	April	May	June	July	Aug.	Sept.	Oct.	Nov.	Dec.
						Means						
Chicama	17.4	18.9	18.6	17.9	17.5	17.2	16.7	16.2	15.8	15.5	15.6	16.2
Offshore	23.3	24.3	24.5	23.4	21.9	20.6	19.4	18.8	18.3	18.7	19.8	21.2
						Standard Deviations						
Chicama	2.0	2.0	1.6	1.8	2.0	1.8	1.2	0.8	0.7	0.9	1.1	1.7
Offshore	1.0	1.0	1.2	1.4	1.5	1.5	1.4	1.2	0.9	0.9	0.9	0.9
						Skewness Coefficients						
Chicama	1.2	0.7	1.5	2.1 0.5*	2.3 0.9*	2.5 0.8*	1.1	0.9	0.2	0.5	2.2	1.7
Offshore	0.7	0.7	0.9	1.2	1.2	1.3	1.3	1.1	0.6	0.6	0.8	0.8

Statistics are based on 1931–1986 for Puerto Chicama and on 1920–1939 and 1949–1986 for offshore.
*Values exclude data from 1982–1983.

TABLE 2. Lag-Autocorrelation Coefficients × 100 for Puerto Chicama SST as a Function of Month, Based on the Period 1931–1986

	Feb.	March	April	May	June	July	Aug.	Sept.	Oct.	Nov.	Dec.	Jan.	Feb.	March	April	May	June	July	Aug.	Sept.	Oct.	Nov.
Jan.	62	47	36	35	35	14	10	20	25	19	4	16	7	5	13	11	7	−1	0	0	6	−4
Feb.		76	56	61	61	55	45	51	40	19	23	18	4	−6	−9	−15	−20	−24	−20	−17	−19	−17
March			82	81	75	63	58	61	49	32	34	26	13	−8	−16	−22	−28	−34	−31	−22	−19	−14
April				93	85	68	59	54	50	33	32	14	14	−4	−12	−17	−19	−19	−18	−11	−12	−11
May					94	77	66	66	62	42	42	27	11	−5	−12	−19	−21	−25	−24	−15	−13	−12
June						85	71	66	61	37	40	22	5	−6	−11	−19	−21	−23	−22	−15	−12	−9
July							89	81	71	49	59	35	18	7	−1	−10	−14	−19	−16	−4	−8	−6
Aug.								89	74	50	58	34	16	1	−5	−12	−16	−18	−14	0	−6	−4
Sept.									83	61	64	49	19	4	0	−7	−13	−17	−13	5	3	5
Oct.										84	76	63	32	30	25	20	18	4	3	20	23	19
Nov.											85	75	45	45	44	41	38	8	3	19	20	11
Dec.												81	48	43	32	28	24	3	0	11	11	7

The reduction of the SST anomalies during the cold season relative to the warm season may be related to the annual cycle of mixed layer depth. The mixed layer is deepest (around 40–60 m) and the stratification in the upper 100 m is weakest during the cold season [*Wyrtki*, 1964]. Thus SSTs should be relatively insensitive to anomalous surface heating and vertical mixing during the cold season. However, during the warm season, when the mixed layer is shallow (around 20 m) and the stratification below the mixed layer is strong, anomalous net surface heating and vertical mixing can cause large changes in SST. It should be noted that during major El Niño events sea level height anomalies along the Peru coast diminish during the cold season [*Wyrtki*, 1975], suggesting a more dynamically oriented interpretation of the corresponding SST anomalies.

The monthly coefficients of skewness for Puerto Chicama and offshore SST are listed in Table 1. (The coefficient of skewness (k) is defined as the third moment coefficient divided by the cube root of the variance). If k exceeds 0.64, the distribution is significantly different (at the 95% confidence level) from a normal distribution for a sample size of 60. The positive skewness exhibited by the SST series is readily apparent in the frequency distributions shown in Figures 1 and 2. It is evident from Table 1 that the positive skewness is highly significant during November–January and March–August at Puerto Chicama and April–August offshore. (If we disregard the extreme anomalies associated with the 1982–1983 El Niño, the skewness for Chicama drops to around 0.8 during April–June but is still highly significant.) In contrast, the frequency distribution for SST in the central equatorial Pacific exhibits negligible skewness [*Wright et al.*, 1987].

Tables 2 and 3 show the autocorrelations as a function of calendar month for SST anomalies at Puerto Chicama and offshore, respectively. These correlation functions are based on unsmoothed monthly mean anomalies. The 1-month lag autocorrelations for Puerto Chicama SSTs exhibit a pronounced seasonal variation, with maximum values in April and May, and minimum values in January and February. In a statistical sense, the time series of January SST anomalies accounts for only about 40% of the variance of the February SST anomalies, whereas the SST anomalies in May explain over 90% of the variance of those in June. Warm season (February–June) anomalies tend to persist through the subsequent cool season (July–November), but there is much less "memory" from the cool season into the subsequent warm season. It is evident that the January–February period is critical for the subsequent evolution of the Puerto Chicama SSTs. The overall pattern of the autocorrelations is similar for offshore SST, but the 1- to 3-month lag correlations are substantially higher at all seasons and the "lapse in memory" is not as sharply concentrated in the January–February interval. It should be noted that these statistics do not necessarily characterize all years individually: in particular, coastal SST anomalies during two of the strongest El Niño events (1982–1983 and 1940–1941) began in the cold season and persisted into the following warm season. We have computed autocorrelation statistics for non–El Niño years separately (not shown) and found that the autocorrelation coefficients are similar during the cold season but are generally lower at all lags during the warm season when El Niño years are excluded from the calculation.

Figure 3 shows the time series of monthly mean SSTs at Puerto Chicama during 1925–1986, together with the mean annual cycle for the period 1950–1979. SST anomalies larger than 1°C are shaded. The shape of the mean annual cycle

TABLE 3. Lag-Autocorrelation Coefficients × 100 for Offshore SST as a Function of Month, Based on the Periods 1921–1939 and 1948–1986

	Feb.	March	April	May	June	July	Aug.	Sept.	Oct.	Nov.	Dec.	Jan.	Feb.	March	April	May	June	July	Aug.	Sept.	Oct.	Nov.
Jan.	86	72	53	48	44	36	32	34	35	31	27	16	12	5	4	−4	−8	−8	−16	−5	−7	1
Feb.		91	75	70	66	59	56	53	55	46	43	36	24	10	1	−7	−11	−13	−21	−11	−12	−6
March			90	85	78	71	67	61	61	50	45	36	21	7	−3	−12	−17	−19	−25	−12	−11	−1
April				94	88	82	76	68	64	53	45	34	24	13	2	−7	−11	−12	−19	−11	−7	2
May					96	91	86	77	71	61	54	42	29	16	6	0	−4	−6	−15	−8	−6	3
June						96	91	82	75	63	55	45	32	17	7	0	−3	−5	−15	−7	−5	4
July							94	84	76	64	56	47	35	18	8	0	0	−2	−14	−7	−6	2
Aug.								90	87	71	65	56	42	25	13	6	4	−1	−10	−7	−4	1
Sept.									94	85	77	67	49	35	25	14	11	5	−2	0	4	10
Oct.										92	86	76	57	40	28	18	14	5	−1	0	5	10
Nov.											95	83	67	51	38	33	30	22	16	16	20	27
Dec.												93	77	58	43	39	37	29	24	26	30	32

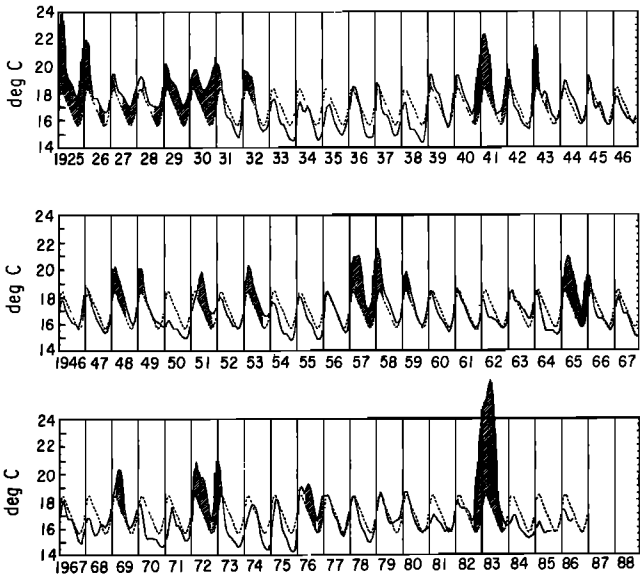

Fig. 3. Time series of monthly SST at Puerto Chicama during 1925–1986 (solid curve) superimposed upon the mean annual cycle of Puerto Chicama SST based on the period 1950–1979 (dashed curve). Monthly anomalies in excess of 1°C are shaded. Anomalies have been smoothed with a three-point binomial filter. Vertical lines mark January of each year.

curve would not be noticeably altered if El Niño years had been left out of the monthly averages. We have reason to suspect that the temperatures during 1925–1930 are biased toward the high side: The offshore SST anomalies, which otherwise agree well with Puerto Chicama values, run about 1°C lower than the Puerto Chicama SST anomalies during this period. (The correlation coefficient between monthly anomalies of Puerto Chicama and offshore SSTs, smoothed with a three-point binomial filter, is 0.86 for the period 1931–1986.) Despite these reservations, we have confidence in the short-term El Niño signal superimposed on this probable bias.

All periods of SST anomalies above 1°C (the shaded intervals in Figure 3), except 1927–1928, 1942, and 1949, correspond to El Niño events as identified by *Quinn et al.* [1978]. (Quinn et al.'s criteria for El Niño events consist of a wide variety of climatic indicators, including above normal SSTs and rainfall along the coasts of Ecuador and Peru and in the central and eastern equatorial Pacific, low Southern Oscillation index, and disruption of the marine ecosystem off the coast of Peru.) The well-known irregularity of El Niño occurrences is apparent in Figure 3: El Niño events may occur as close as 1 or 2 years apart, or longer than 6 years apart as in the decade of the 1930s. The duration of El Niño events is also variable: an event may last from a few months (e.g., in 1932, 1943, and 1949) to a full year (e.g., in 1957, 1965, 1972, and 1982–1983). It can be seen from Figure 3 that El Niño frequently sets in abruptly during February (e.g., in 1932, 1953, 1957, 1965, and 1972); El Niño has also begun in January (1939 and 1943), March (1953), and April (1969) and around October (1982, 1940, and 1930). These aspects of past El Niño events have been noted by previous authors [e.g., *Quinn et al.*, 1978].

The coastal SST anomalies associated with El Niño are invariably most pronounced during the warm months, December through June (see Figure 1). Therefore those events that begin around February and last 1 year appear as two successive peaks in the coastal SST anomalies, the first typically in February through June and the second in December through February. However, if the monthly SST anomalies are normalized by their standard deviations, this double peak structure becomes less pronounced. Hence significant positive SST anomalies are nearly always present during the cold season of El Niño years, but their magnitudes are usually less than 1°C.

The time series of offshore SST [see *Rasmusson and Carpenter*, 1982, Figure 11] lacks the pronounced second (December–

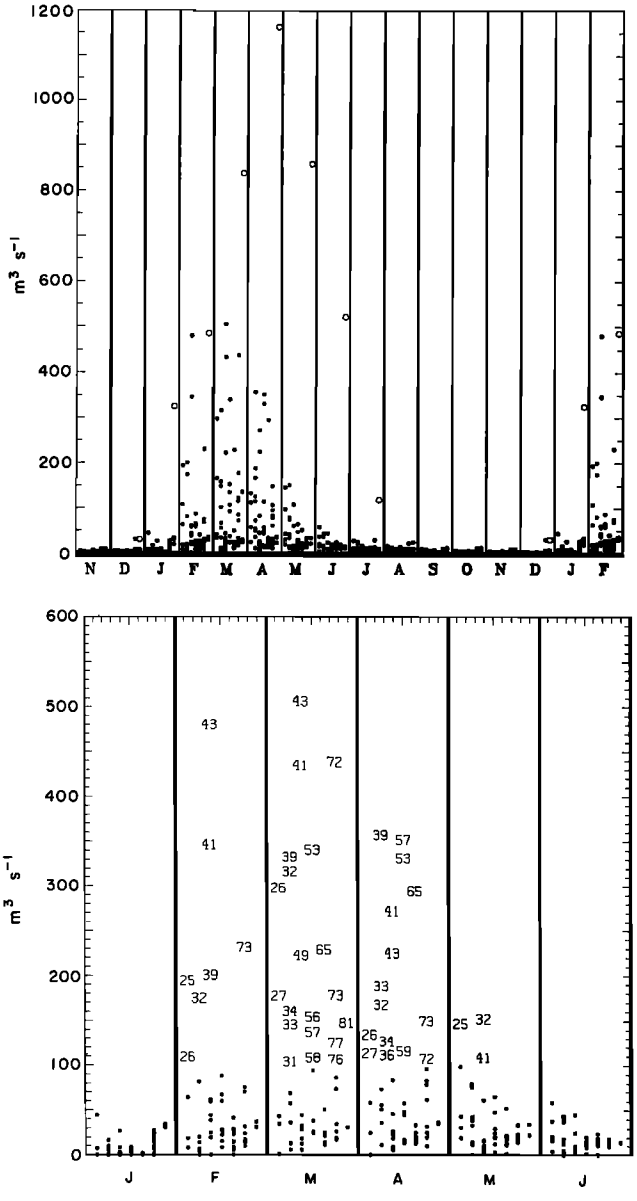

Fig. 4. (*a*) Distribution of discharge (in cubic meters per second) from the Piura River at Piura (5°S, 81°W) during 1925–1983, stratified by month. Each dot marks the median discharge for an individual year-month. Each column of dots within a given calendar month represents a particular decade; i.e., the first (last) column of dots contains data for the 1920s (1980s). November through February are repeated. Data for November 1982 through July 1983 are marked by open circles. (*b*) As in Figure 4*a* but for January through June only, 1925–1981. Discharges greater than 100 $m^3 s^{-1}$ are identified by the last two digits of the year in which they occurred. Data are missing for March and April 1925 and for 1950–1951. Note that data for 1982–1983 have been omitted.

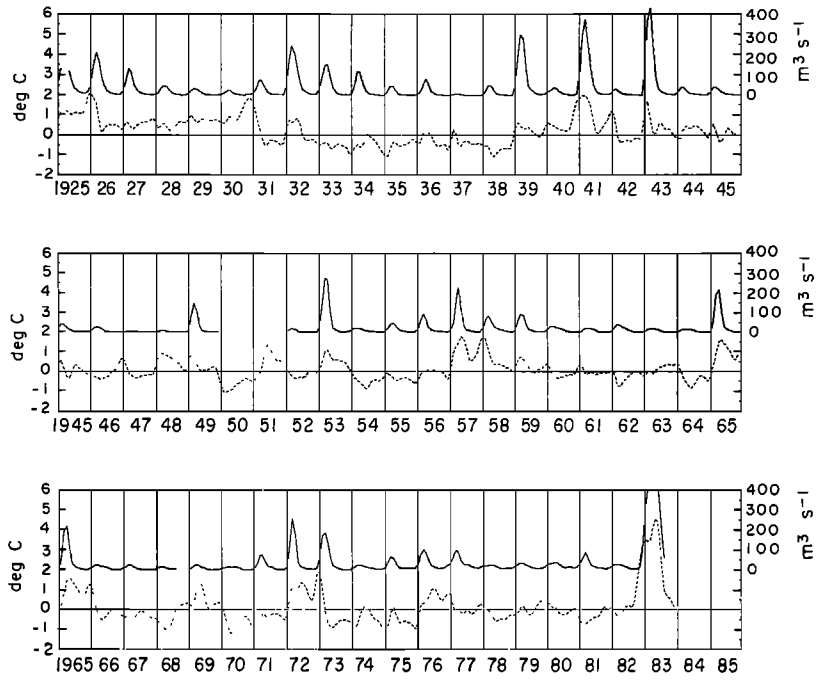

Fig. 5. Time series of monthly discharge (in cubic meters per second) of the Piura River at Piura (solid curve) and SST anomalies (in degrees Celsius) at Puerto Chicama (dashed curve) during 1925–1983. The data have been smoothed with a three point binomial filter. Vertical lines mark January of each year. Note that discharge values are missing for March and April 1925, and for 1950–1951; data offscale during 1983 are omitted.

February) peaks present in the Puerto Chicama record. Offshore SST remains above normal during these months toward the end of El Niño events, but the anomalies tend to be much smaller than on the coast (see Figure 2).

3. Piura River Runoff and its Relation to Puerto Chicama SST

We use the median discharge of the Piura river at Piura (5°S, 81°W) as a measure of rainfall integrated over a drainage basin roughly 7500 km^2 in extent. The low-lying Piura River receives almost no snowmelt from the Andes (R. Mugica, personal communication, 1987). This discharge record covers the period 1925–1983 and was kindly provided by R. Mugica of the Universidad de Piura. The streamflow recorder was swept away by floods during March 1925 [*Murphy*, 1926], and data are also missing for 1950–1951 (see *Horel and Cornejo-Garrido* [1986] for further discussion of this record). It should be noted that annual rainfall totals at individual stations in the lowland plains of Peru and Ecuador are only moderately well correlated with annual runoff of the Piura River. The correlation coefficients between anomalies of annual totals of Piura River runoff and precipitation at Guayaquil (2.1°S, 80°W), Talara (4.5°S, 81°W), Lambayeque (6.6°S, 80°W), and Chiclayo (6.8°S, 80°W) are 0.77, 0.23, 0.64, and 0.45, respectively, based on the period 1950–1979.

Figure 4*a* shows the distribution of the median discharge of the Piura River at Piura as a function of month during 1925–1983. On average, the largest flows of the Piura River occur from February through May. There is a lack of appreciable streamflow during August–December, even in El Niño years. Record flows occurred in January 1983 and from March through July 1983. Figure 4*b* shows the distribution of Piura River discharge for January–June only, 1925–1981; months of high discharge are labeled by year.

It is interesting to note that the onset of the rainy season in northern coastal Peru occurs when SSTs are already at their seasonal maximum. Precipitation is much heavier in April than in January; yet SSTs along northern Peru are nearly identical for these 2 months. Other factors besides SST, such as low-level wind convergence and static stability, must play a strong role in determining the timing of the rainy season in northern Peru.

Figure 5 shows the time series of Puerto Chicama SST anomalies and Piura River discharge at Piura, smoothed with a three-point binomial filter, during 1925–1983. It can be seen that many years of above (below) normal SST are accompanied by above (below) normal streamflow. Notable exceptions are 1939 (very high runoff but only small positive SST anomalies), 1948 and 1969 (negligible runoff but substantial positive SST anomalies), and 1933 and 1934 (below normal SSTs but above average runoff). The prolonged El Niño events of 1925, 1957, and 1972 appear to have enhanced the runoff in the subsequent calendar year, but the prolonged event of 1965 did not produce substantial runoff in 1966. Piura River discharge in 1943 was one of the largest on record, yet Puerto Chicama SST was above normal for only the first 2 months of the year. In contrast, SST was above normal from May to December in 1976, but runoff was only slightly enhanced.

It appears that the precipitation response is sensitive to the timing of the SST anomaly associated with El Niño. Figure 6 shows the runoff for years with above normal Puerto Chicama SST during December–February but not later (1926, 1943, 1958, 1966, 1973, and 1977) and years with above normal Puerto Chicama SST during February–June but not before

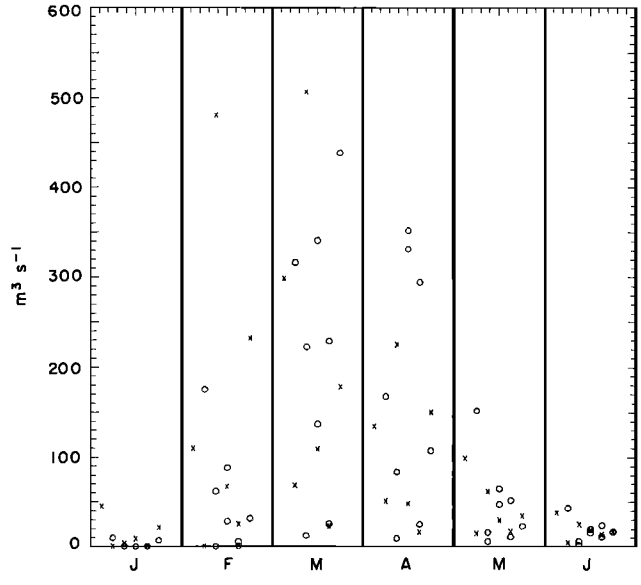

Fig. 6. Distribution of discharge (in cubic meters per second) from the Piura River at Piura during January–June, 1925–1981. Years with above normal SST at Puerto Chicama during December–February but not later (1926, 1943, 1958, 1966, 1973, and 1977) are marked by crosses; years with above normal SST at Puerto Chicama during February–June but not before (1932, 1948, 1949, 1953, 1957, 1965, 1969, and 1972) are marked by open circles.

(1932, 1948, 1949, 1953, 1957, 1965, 1969, and 1972). The latter group of years shows a greater enhancement of rainfall toward the end of the wet season (March–April), while the former group exhibits a more modest enhancement of runoff (with the exception of 1943) near the onset of the wet season.

Finally, it should be noted that on interannual time scales, Piura river runoff is more closely related to Puerto Chicama SST than to offshore SST, Darwin, Australia, sea level pressure (SLP), or Tahiti SLP. The correlation coefficients between anomalies of January–June averages of Piura River runoff and seasonal averages of Puerto Chicama SST, offshore SST, Darwin SLP, and Tahiti SLP are 0.74, 0.58, 0.40, and −0.39, respectively, for the period 1931–1983.

4. El Niño and the Southern Oscillation

Seasonal anomalies of Darwin SLP are highly correlated (correlation coefficients near 0.9 for the period 1950–1979) with seasonal anomalies of SST, rainfall, and zonal wind in the central equatorial Pacific (160–170°W) and with the conventional Southern Oscillation indices (e.g., Tahiti minus Darwin SLP) [*Wright et al.*, 1987]. Therefore Darwin SLP anomalies can be used as an indicator of the state of the Southern Oscillation and the associated large-scale climatic changes in the central equatorial Pacific.

Smoothed monthly anomalies of Darwin SLP and Puerto Chicama SST for the period 1925–1985 are shown in Figure 7. SST anomalies are plotted only when they exceed 1°C. The monthly SST and SLP anomalies have been smoothed with single and double applications of a 3-point binomial filter respectively. It is evident that El Niño events (indicated by shading) occur in a variety of juxtapositions with episodes of above normal Darwin SLP. El Niño events have occurred in advance of episodes of positive Darwin SLP anomalies (as in 1925, 1951, 1953, 1957, 1965, and 1972) and just subsequent to them (as in 1930–1931, 1940–1941, and 1982–1983). It is notable that the 1950–1975 period, which was the basis for the *Rasmusson and Carpenter* [1982] ENSO composite, was dominated by events belonging to the former group.

It is also evident from Figure 7 that El Niño events have occurred in the absence of pronounced positive Darwin SLP anomalies (as in 1932 and 1943). The El Niño events of 1932

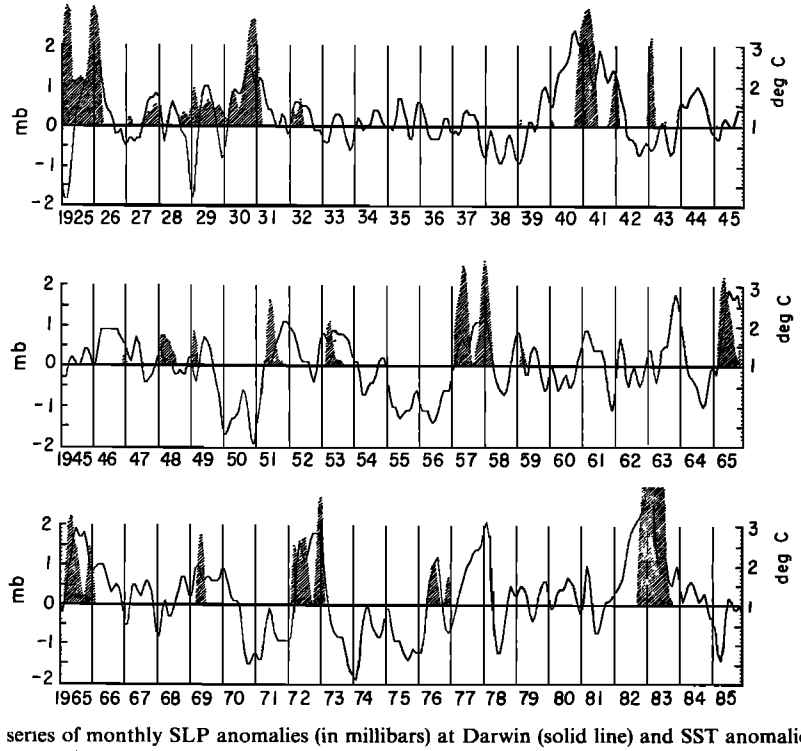

Fig. 7. Time series of monthly SLP anomalies (in millibars) at Darwin (solid line) and SST anomalies in excess of 1°C at Puerto Chicama (shaded) during 1925–1985. The SST and SLP anomalies have been smoothed with single and double applications of a three-point binomial filter respectively. Note that the origin of the ordinate for the SST anomalies is 1°C. Vertical lines mark January of each year. Values offscale during 1982–1938 are not plotted.

and 1943 were associated with heavy rains and severe flooding along the coastal plain of northern Peru [*Sheppard*, 1933; *Alpert*, 1946] and thus rank as being comparable in importance to the other major (and perhaps more familiar) events of 1925–1926, 1940–1941, 1957–1958, and 1972–1973. Offshore SSTs were well above normal during 1932; the offshore SST index was not calculated in 1943 for lack of observations. The lack of a Darwin SLP signal in 1932 and 1943 is consistent with observed surface pressures in these years at other Australian and Indonesian stations and with the lack of above normal SST and rainfall in the central equatorial Pacific (not shown).

Conversely, it is also evident from Figure 7 that the major negative swings of the Southern Oscillation that occurred in 1963 and 1977 were not accompanied by El Niño events. A similar lack of correspondence was observed in 1923, when Darwin SLP was well above normal (not shown). The pronounced peaks in Darwin SLP anomalies during 1923, 1963, and 1977 were attended by above normal SSTs and rainfall in the central equatorial Pacific and below normal SLPs at Tahiti (not shown), yet eastern Pacific SSTs (coastal and offshore) and rainfall were about average.

Hence El Niño and the Southern Oscillation are more loosely coupled than the studies of *Bjerknes* [1966] and *Rasmusson and Carpenter* [1982] would imply. Evidently, there are strong local controls on the climate of the eastern equatorial Pacific that sometimes transcend the influence of the Southern Oscillation. Year-to-year variations in coastal SSTs may not necessarily be reflected in swings of the Southern Oscillation and associated large-scale climatic changes in the central equatorial Pacific, but they could have an important influence on local rainfall. An understanding of the local climatic controls in the eastern equatorial Pacific would constitute an important step toward a full explanation of the ENSO phenomenon.

Acknowledgments. We would like to thank Kay Dewar for her help in preparing the figures. This work was supported under grant 8318853 from the National Science Foundation's Climate Dynamics Program Office. The suggestions and comments of the anonymous reviewers helped improve the manuscript.

REFERENCES

Alpert, L., Weather over the tropical eastern Pacific Ocean, 7 and 8 March 1943, *Bull. Am. Meteorol. Soc.*, *27*, 384–397, 1946.

Barnett, T. P., Variations in near-global sea level pressure, *J. Atmos. Sci.*, *42*, 478–501, 1985.

Berlage, H. P., The Southern Oscillation and world weather, *Meded. Verh. K. Ned. Meteorol. Inst.*, *88*, 152 pp., 1966.

Bjerknes, J., "El Niño" study based on analysis of ocean surface temperatures 1935–57, *Inter. Am. Trop. Tuna Comm. Bull.*, *5*(3), 219–271, 1961.

Bjerknes, J., A possible response of the atmospheric Hadley circulation to equatorial anomalies of ocean temperature, *Tellus*, *18*, 820–829, 1966.

Brooks, C. E. P., and H. W. Braby, The clash of the trades in the Pacific, *Q.J.R. Meteorol. Soc.*, *47*, 1–13, 1921.

Cane, M. A., Oceanographic events during El Niño, *Science*, *222*, 1189–1195, 1983.

Carillo, C. N., Disertación sobre las corrientes oceanicas, *Bol. Soc. Geogr. Lima*, *2*, 1892.

Eguiguren, D. V., Las nuivas de Piura, *Bol. Soc. Geogr. Lima*, *4*, 241–258, 1894. (English translation, R. S. Quiroz, Climate Analysis Center, Natl. Meteorol. Center, Natl. Oceanic and Atmos. Admin., Washington, D. C., July 1984. Available from translator.)

Fu, C-G., H. F. Diaz, and J. O. Fletcher, Characteristics of the response of sea surface temperature in the central Pacific associated with warm episodes of the Southern Oscillation, *Mon. Weather Rev.*, *114*, 1716–1738, 1986.

Guillén, O., and R. Calienes, Upwelling off Chimbote, in *Coastal Upwelling, Coastal and Estuarine Sci.*, vol. 1, edited by F. A. Richards, pp. 312–326, AGU, Washington, D. C., 1981.

Gunther, E. R., A report on oceanographical investigations in the Peru Coastal Current, *Discovery Rep.*, *13*, 107–276, 1936.

Hildebrandsson, H. H., Quelques recherches sur les centres d'action de l'atmosphere, *K. Sven. Vetenskapsakad. Handl.*, *29*, 33 pp., 1897.

Horel, J. D., and A. G. Cornejo-Garrido, Convection along the coast of northern Peru during 1983: Spatial and temporal variation of clouds and rainfall, *Mon. Weather Rev.*, *114*, 2091–2105, 1986.

Kidson, J. W., Tropical eigenvector analysis and the Southern Oscillation, *Mon. Weather Rev.*, *103*, 187–196, 1975.

Lagos, P., T. P. Mitchell and J. M. Wallace, Remote forcing of sea surface temperature in the El Niño region, *J. Geophys. Res.*, this issue.

Lobell, M. J., Some observations on the Peruvian coastal current, *Eos Trans. AGU*, 332–336, 1942.

Lockyer, N., and W. J. S. Lockyer, The behaviour of the short-period atmospheric pressure vatioation over the earth's surface, *Proc. R. Soc. London*, *73*, 457–470, 1904.

Mears, E. G., The ocean current "The Child," *Smithson. Inst. Annu. Rep.*, 245–251, 1943.

Murphy, R. C., Oceanic and climatic phenomena along the west coast of South America during 1925, *Geogr. Rev.*, *16*, 26–54, 1926.

Quinn, W. H., V. T. Neal, and S. E. Antunez de Mayolo, El Niño occurrences over the past four and a half centuries, *J. Geophys. Res.*, this issue.

Quinn, W. H., D. O. Zopf, K. S. Short, and R. T. W. Kuo Yang, Historical trends and statistics of the Southern Oscillation, El Niño, and Indonesian droughts, *Fish. Bull.*, *76*, 663–678, 1978.

Rasmusson, E. M., and T. H. Carpenter, Variations in tropical sea surface temperature and surface wind fields associated with the Southern Oscillation/El Niño, *Mon. Weather Rev.*, *110*, 354–384, 1982.

Schott, G., Der Peru-Strom und seine nordlichen Nachbargebiete in normaler und anormaler Ausbildung, *Ann. Hydrogr. Mar. Meteorol.*, *59*, 161–252, 1931.

Schweigger, E., La "legitima" corriente del Niño, *Bol. Cia. Adm. Guano*, *21*, 255–296, 1945.

Sheppard, G., The rainy season of 1932 in southwestern Ecuador, *Geogr. Rev.*, *23*, 210–216, 1933.

Smith, R. L., A comparison of the structure and variability of the flow field in three coastal upwelling regions: Oregon, northwest Africa, and Peru, in *Coastal Upwelling, Coastal and Estuarine Sci.*, edited by F. A. Richards, pp. 107–118, AGU, Washington, D. C., 1981.

Trenberth, K. E., Spatial and temporal variations of the Southern Oscillation, *Q.J.R. Meteorol. Soc.*, *102*, 639–653, 1976.

Troup, A. J., The Southern Oscillation, *Q.J.R. Meteorol. Soc.*, *91*, 490–506, 1965.

Walker, G. T., and E. W. Bliss, World Weather V, *Mem. R. Meteorol. Soc.*, *4*, 53–84, 1932.

Wooster, W. S., El Niño, *CalCOFI Rep. 7*, pp. 43–45, Calif. Coop. Ocean. Fish. Invest., Univ. of Calif., San Diego, La Jolla, 1960.

Wright, P. B., J. M. Wallace, T. P. Mitchell, and C. Deser, Correlation structure of the El Niño/Southern Oscillation phenomenon, *Mon. Weather Rev.*, 1987.

Wyrtki, K., El Niño—The dynamic response of the equatorial Pacific Ocean to atmospheric forcing, *J. Phys. Oceanogr.*, *5*, 572–584, 1975.

C. Deser and J. M. Wallace, Department of Atmospheric Sciences, AK-40, University of Washington, Seattle, WA 98195.

(Received March 2, 1987;
accepted March 25, 1987.)